

Diagnostics and Impulse Performance of Laser-Ablative Propulsion

Akihiro Sasoh^a, Koichi Mori^a, Kohei Anju^b, Koji Suzuki^b, Masaya Shimono^b and Keisuke Sawada^b

^a*Department of Aerospace Engineering, Nagoya University, Furo-cho, Chikusa-ku, Nagoya 464-8603, Japan*

^b*Department of Aerospace Engineering, Tohoku University, 6-6-2 Aramaki-Aza-Aoba, Sendai 980-8579, Japan*

Abstract. Pressure time variations and associated flows induced by pulsed laser ablation were experimentally studied using the Velocity Interferometer System for Any Reflector (VISAR) and framing Schlieren visualization. The combination of either aluminum or polyacetal target and TEA CO₂ laser pulse were examined. The VISAR measurement resolved that the pressure modulated from the laser power variation in the impulse generation processes. Integrated impulse induced by repetitive CO₂ laser pulses was measured using a torsion-type impulse balance. The effect of the ambient pressure was significant. The measured impulse characteristics were closely associated with target surface morphology and fluid dynamics.

Keywords: Laser ablation, In-tube propulsion, Ram accelerator, Impulse

PACS: 42.62.-b, 47.40.-Nm

INTRODUCTION

Ablative laser propulsion^{1,2} is a feasible and promising laser propulsion technology. However, the impulse generation mechanisms were not clearly understood due to the lack of detailed diagnostics. In space a laser beam interacts with the target and the resulting ablation plume. The interaction involves complicated physical processes such as electrical breakdown, phase change, ionization, laser power absorption, plume jet dynamics, heat conduction, radiative heat transfer etc. In the presence of ambient air, the complexity becomes even greater because the air itself can absorb the laser energy, and shock and expansion waves are generated thereby inducing more complicated flow dynamics. Watanabe et al.³ through their free-flight experiments obtained complicated but useful impulse performance for polyacetal (POM) subjected to a TEA CO₂ laser pulse; in an appropriate fluence range the impulse was larger at low ambient pressures than at the atmospheric pressure. In the beginning part of this paper, we have obtained time variation of laser-ablative impulse and associated flows using the Velocity Interferometer System for Any Reflector (VISAR)⁴ and framing Schlieren visualization.

Phipps et al.⁵ proposed formulae for a laser-ablative impulse by integrating experimental and theoretical data on metals and polymers, showing that an optimum intensity exists to maximize the momentum coupling coefficient, C_m . Pakhomov et al.⁶⁻⁸ investigated laser-impulse characteristics of various metals; they also highlighted the effect of ambient air pressure on the impulse. Watanabe et al.⁹ determined an optimum condition with respect both to the laser fluence and the ambient pressure when irradiating a target made of polyacetal (POM) with a TEA CO₂ laser pulse the combination of which gave the most favorable impulse performance among the polymers tested. These results imply that in order to optimize propulsion performance, irradiating with a giant pulse of excessively high fluence should be avoided; if the laser irradiation area on a target is not large enough, C_m can be maximized by repetitively irradiating laser pulses with the energy corresponding to the optimum fluence. If the total impulse increases almost linearly with the number of laser pulses of constant energy, we can remotely obtain a desired value of impulse in space. The same principle applies to laser-powered space debris de-orbiting.¹⁰ At the later part of this paper, we will experimentally investigate the impulse characteristics of POM to repetitive TEA CO₂ laser pulses irradiated onto a fixed spot.

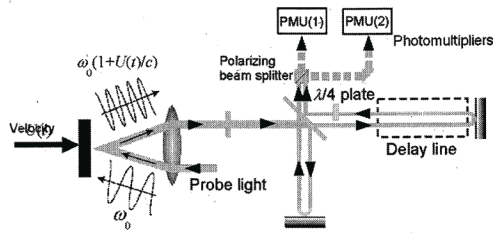


FIGURE 1. Operation principle of VISAR

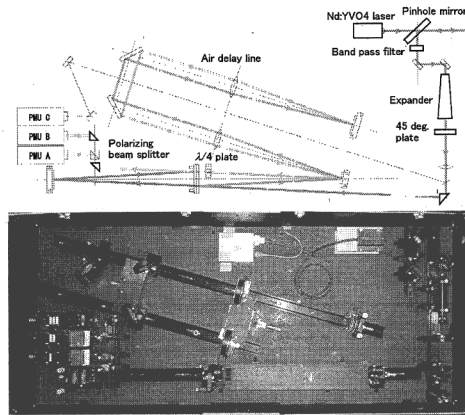


FIGURE 2. VISAR, 20.0 m/s/fringe

TEMPORAL LOCAL PRESSURE MEASUREMENT

The velocity interferometer system for any reflector (VISAR)^{4,11} is a Michelson-type interferometer which has been used in hypervelocity impact study to determine the equation of state of material under a high pressure. Figure 1 illustrates its operation principle. As a probe light, a CW, single-mode laser light is incident on the surface of a target sheet. The light is diffusively reflected from the surface, and introduced to the interferometer. In the interferometer, the reflected light is split into two optical path the optical length of which differs by ΔL from each other. The reflected light has a Doppler shift which is linear with respect to the surface velocity. The two split beams interfere with each other, thereby producing a beat signal. The phase of the beat is a linear function of the velocity. Figure 2 shows the arrangement of the VISAR. In this case, the optical delay is generated by a 4-m-long optical path in the atmospheric air. In order to increase the fringe constant, a water delay is used, obtaining 99.8 m/s/fringe. Figure 3 shows an example of VISAR signals, the corresponding Lissajous figures and reduced velocity history.

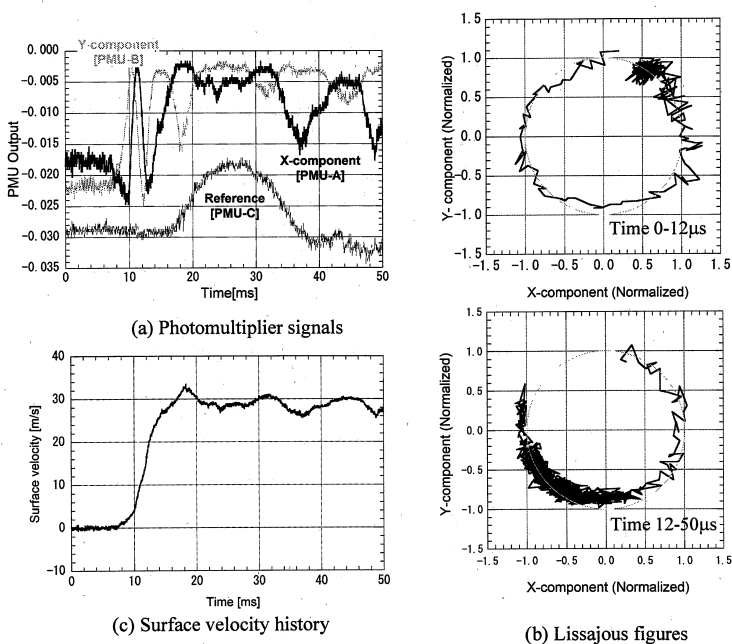
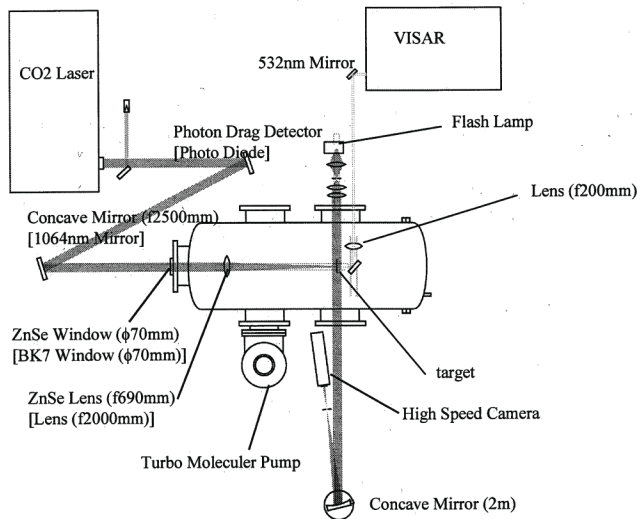
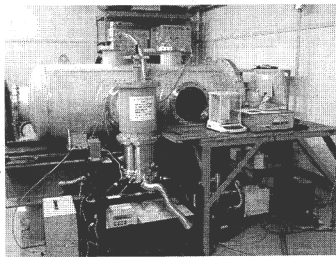


FIGURE 3. Example of VISAR signals and velocity history.

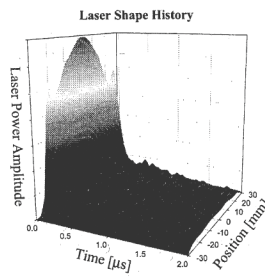
In this study, TEA CO₂ laser (wavelength; 10.6 μm l, SLCR-Lasertechnik GmbH: ML205) pulses were introduced to the vacuum chamber (inner dia.; 0.7 m, length 1.8 m) after being reflected from two collimating molybdenum mirrors and sent through a ZnSe plane-convex lens of focal length of 1.07 m. The laser beam has a diameter of 55 mm at the oscillator exit. The energy of a single laser pulse was measured with an energy meter (ED-500LIR, Gentec Electro-Optics Inc.); time variation of the intensity was measured with a photon-drag sensor (B749, Hamamatsu Photonics). For a total energy of 10 J, the laser pulse had a primary peak intensity of 60 MW/cm² full-width at half maximum of 170 ns with 90 % of the total energy output within 3.1 μs .



(a) Whole system



(b) photograph of vacuum chamber



(c) laser power profile.....

FIGURE 4. Setup for VISAR measurement

Figure 4 shows the experimental setup for the VISAR measurement. A square target 100 mm on a side was cleaned with ethanol, and introduced into the vacuum chamber (inner diameter; 0.7 m, length; 2.0 m). The vacuum chamber was evacuated using a turbo-molecular pump (TMP-2003LM, Shimazu, 2000 L/s for N_2), which in turn was backed by a rotary pump (T2033SD, Alcatel, 500 L/min). The target was sandwiched by an aluminum holder at its upper and lower sides. For visualization, the left and right sides were left free. A laser pulse was directed onto the front surface (left surface in Fig. 4(a)) of the target. The target is made either of aluminum or polyacetal (POM). Further details of the pressure measurement using the VISAR are provided elsewhere.¹²

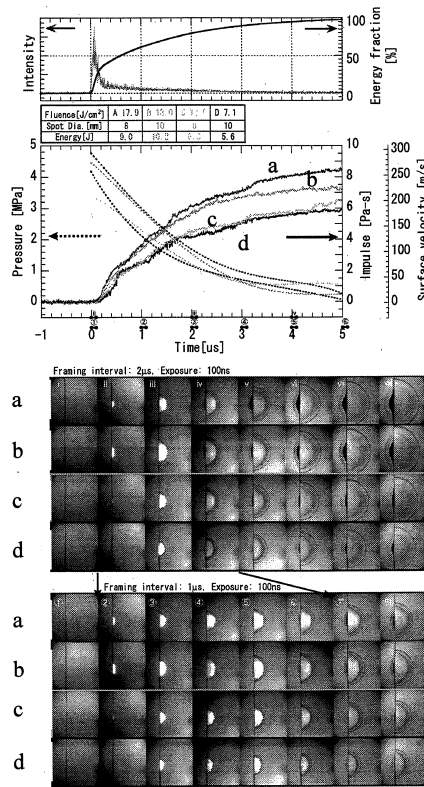


FIGURE 5. Laser power profile, surface velocity and framing Schlieren pictures, Aluminum target, $P_0=100$ kPa, (a) $E=9.0$ J, $d=8$ mm (17.9 J/cm²), (b) $E=10.2$ J, $d=10$ mm (13.0 J/cm²), (c) $E=6.3$ J, $d=8$ mm (12.5 J/cm²), (d) $E=5.6$ J, $d=10$ mm (7.1 J/cm²).

Figure 5 shows time variations of laser intensity, surface velocity, and flow visualization of the laser plasma and ablation plume in the case of POM target in the atmospheric air. The fluence was varied by varying a laser pulse energy and/or the spot diameter. As seen the velocity histories, the impulse continues to increase even after the primary intensity peak. In the presence of the atmospheric air, when the laser-induced plasma expands toward the surroundings a hemispherical shock wave is driven. The post-shock pressure lasts in a period much longer than the FWHM of the laser intensity. The surface velocity is an increasing function of the fluence.

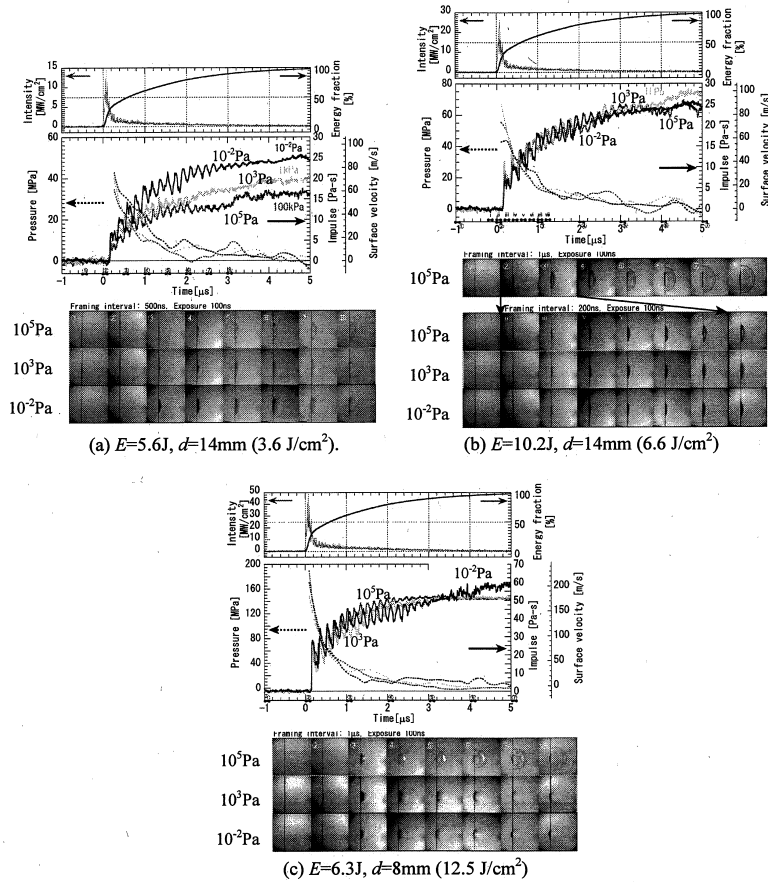


FIGURE 6. Laser power profile, surface velocity and framing Schlieren pictures, POM target.

Figure 6 shows the cases of POM target with different fluence. In each velocity history, the signal of reverberation is superimposed on the velocity of the center of mass. Tracing the mean value in each reverberation reasonably yield the averaged velocity history. In these cases, the ambient pressure, P_0 , is also varied. The fluence level is relatively low. Data with even higher fluence is presented elsewhere.¹² At the fluence of 3.6 J/cm^2 , the terminal value of the impulse increases with decreasing P_0 , whereas in other conditions C_m depends on P_0 in a complicated manner. Yet, overall, the presented P_0 -dependence of the impulse is consistent with that is reported by Watanabe et al.³

IMPULSE AGAINST REPETITIVE PULSES

Figure 7 shows the schematic diagram of the experimental setup. The impulse balance was set in the vacuum chamber with its arm parallel to the chamber axis. For details of the impulse balance refer to Ref. 13. The target was made of ployacetal (POM), 10 mm in thickness, and 22 mm in diameter on the incident surface, flush-mounted on a 100 mm dia. aluminum holder plate which was attached to the side face of the balance arm. The laser beam was irradiated normal to the target surface. Before laser pulse irradiance, the target surface was not mechanically or chemically processed -- only cleaned using ethanol. The pumps were kept in operation even during laser pulse irradiations.

Figure 8 shows the variation of C_m as the function of the accumulated number of pulses from the virgin surface, N . According to Ref. 13, the impulse performance was degraded in the first several shots. In order to eliminate the degraded performance. In each run the first ten pulses were regarded as 'cleaning shots;' the impulse performance was not evaluated. Impulse performance was measured in different burst modes. After a bundle of ΔN laser pulses were irradiated at a repetition frequency of 50 Hz, the target was kept intact during for more than three minutes. This burst cycle was repeated until the total number of pulses, N , amounted to 110.

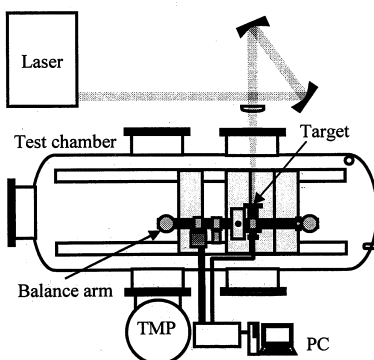


FIGURE 7. Setup for ballistic balance measurement

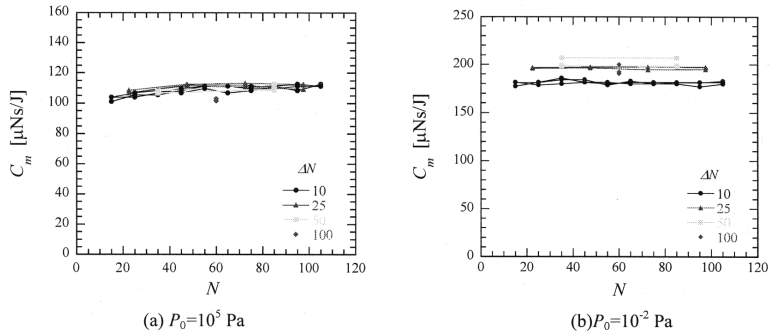


FIGURE 8. C_m vs. N , $E = 6.74 \text{ J}$, $d = 8.6 \text{ mm}$, $(\phi = 12.0 \text{ J/cm}^2)$

Figure 8 shows the variations of C_m measured for a fluence of 12.0 J/cm^2 . A higher level of C_m was obtained for $P_0 = 10^{-2} \text{ Pa}$ than for $P_0 = 10^5 \text{ Pa}$. This tendency quantitatively agrees with Watanabe et al.'s free flight experiment³ and those of the above-mentioned VISAR measurement. However, quantitative agreement in the impulses are not obtained between Figs. 6 and 8. In Fig. 6, the impulse was measured with targets having virgin surface. As is reported in Ref. 13, scatter in C_m is considerably high during the first several shots. Anyway, the impulse performance at the lower pressure was about 1.5 times higher than that under the atmosphere. The effect of burst mode, that is ΔN , is not conclusively clear among the tested runs. In each run shown in Fig. 8, C_m was kept almost constant within 10% variation.

Figure 9 shows the photograph of molded shapes of the crater which was formed after 110 laser pulse irradiations. Fig. 9(a) corresponds to $\Delta N = 100$ shot shown in Fig. 8(a). After the 110 shots, a crater, the radius of which almost equaled to that of the effective laser spot was formed. In this case, the crater acted as an aerodynamic nozzle for the ablation plume, thereby increasing the impulse performance. However, if the crater was too deep as shown in Fig. 9(b), the impulse performance was decreased for $N > 50$, see Fig. 10.

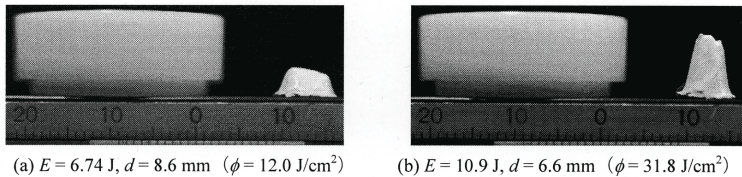


FIGURE 9. Example of ablated volume and crater shape, $P_0 = 10^{-2} \text{ Pa}$, $N = 110$, $\Delta N = 100$.

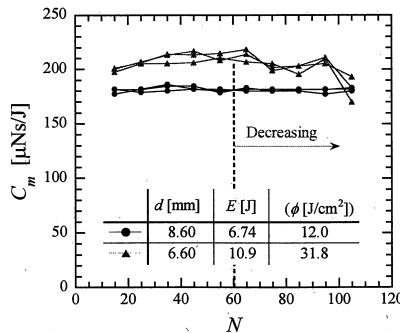


FIGURE 10. C_m vs. N , $P_0=10^{-2}$ Pa, lower; $E = 6.74$ J, $d = 8.60$ mm ($\phi = 12.0$ J/cm²), upper; $E = 10.9$ J, $d = 6.60$ mm ($\phi = 31.8$ J/cm²)

SUMMARY

In this paper, time-resolved diagnostics of ablative laser impulse generation was done using the VISAR. The ablative impulse is time modulated from the irradiated laser power profile; the impulse after the primary power peak has a great contribution to, or even is dominating over, the total value. The impulse performance after several laser pulse irradiations differ from that against the virgin specimen. The morphology of the crater affects the impulse performance. Such characteristics become important in practically controlling the motion of an object in space with repetitively irradiating laser pulses.

ACKNOWLEDGMENTS

We cordially appreciate valuable technical assistances from Technical Division, Graduate School of Engineering, Nagoya University, and Technical Division, Institute of Fluid Science, Tohoku University, in particular from A. Saito and T. Ogawa. Also we acknowledge technical discussions, suggestions and encouragements from T. Ueno, N. Ohnishi and T. Sakai.

REFERENCES

- ¹ A. Kantrowitz, *Astronautics and Aeronautics* **10**, 74-76 (1972).
- ² A. V. Pakhomov, D. A. Gregory, *AIAA Journal* **38**, 725-727 (2000).
- ³ K. Watanabe, K. Mori, A. Sasoh, *Journal of Propulsion and Power*, **22**, 1149-1151 (2006).
- ⁴ L. M. Barker, R. E. Hollenbach, *Journal of Applied Physics* **43**, 4669-4675 (1972).
- ⁵ C. Phipps, et al. *Journal of Applied Physics* **64**, 1083-1096 (1988).
- ⁶ A. V. Pakhomov, M. S. Thompson, W. Swift Jr., D. A. Gregory, *AIAA Journal* **40**, 2305-2311 (2002).
- ⁷ A. V. Pakhomov, J. Lin, R. Tan, *AIAA Journal* **44**, 136-141 (2006).

- ⁸ J. Lin, J. Hughes, A. V. Pakhomov, "Experimental study of coupling coefficients for propulsion on TEA CO₂ Laser," in *Proceedings of Second International Symposium on Beamed Energy Propulsion*, edited by K. Komurasaki, Vol. 702, American Institute of Physics, 2004, pp. 122-128.
- ⁹ K. Watanabe, A. Sasoh, Transaction of Japan Society for Aeronautical and Space Sciences **48**, 49-52 (2005).
- ¹⁰ C. Phipps, "ORION, Challenges and Benefits," in *Proceedings of High-Power Laser Ablation*, edited by C. Phipps, Vol.3343, The International Society for Optical Engineering, Bellingham, WA, 1998, pp.575-582.
- ¹¹ L. M. Barker, K. W. Schuler, Journal of Applied Physics **45**, 3692-3693 (1974).
- ¹² K. Anju, K.. Sawada, A. Sasoh, K. Mori, E. Zaretsky, J. Propulsion and Power, to appear.
- ¹³ A. Sasoh et al., AIAA paper, AIAA-2007-4389 (2007).